A Novel Passive RFID Temperature Sensor

Yousuf Shafiq, John Gibson and Stavros V. Georgakopoulos
Department of Electrical and Computer Engineering
Florida International University
Miami, FL 33174
yshaf001@fiu.edu, jgibs023@fiu.edu, georgako@fiu.edu

Hyun Kim, Cedric P. Ambulo, and Taylor H. Ware
Department of Bioengineering
The University of Texas at Dallas
Richardson, TX 75080
kimhyun@utdallas.edu, cpa160130@utdallas.edu, taylor.ware@utdallas.edu

***Abstract*—A novel passive RFID temperature sensor is proposed in this paper. The sensor utilizes an integrated T-match network (TMN) for matching the antenna to the RFID IC. Furthermore, the sensor detects changes in temperature by shifting its operating frequency. The frequency shifts are accomplished by a 3D printed liquid crystal elastomer (LCE) array that can reversibly actuate depending on the temperature to move the antenna and change its distance from the ground plane.**

Keywords—RFID, temperature sensor, T-match network, liquid crystal elastomer (LCE)

I. Introduction

Many foods and medicines need to be maintained within a temperature range to avoid spoilage [1]. For this reason, a temperature sensor using real-time and battery-less technology is proposed. Moreover, due to standardized communication protocols and non-line-of-sight communication, RFID technology is incorporated.

The proposed sensor uses a planar dipole antenna design with a customized matching technique for a complex conjugate match to the RFID IC [1]. Specifically, the TMN is integrated into the planar dipole antenna [2]. Furthermore, an innovative 3D printed LCE is used to actuate the antenna [3]. As a result, the sensor detects increases in temperature through detectable shifts in its operating frequency. Finally, the design is verified using ANSYS HFSS simulations and measurements.

II. The T-match Network

A. Theory

The TMN serves as a means of impedance matching. Moreover, it is a general form of the folded dipole antenna since the length and/or the diameters of the two legs are not generally the same, refer to Fig. 1.

As a result, the current distribution in each leg depends on the raddii a′ and a. In order to account for this nonuniform current distribution, the current division factor (α) based on the geometry is introduced [4].

$$\alpha = \left(\ln\left(\frac{x}{a'}\right)\right) \Big/ \left(\ln\left(\frac{x}{a'}\right) - \ln\left(\frac{a}{a'}\right)\right) \qquad (0)$$

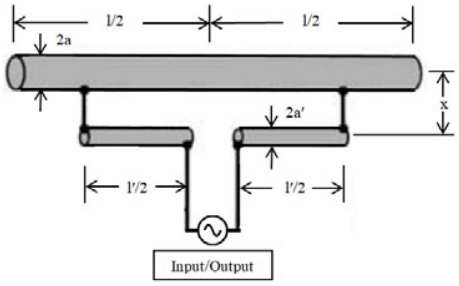

Fig. 1. The T-match model where a′ ≠ a and l′ ≠ l.

A transformer model can suitably represent the TMN. On the load side, there exists an input antenna impedance (Z_{ANT}) of a dipole antenna without any matching network. While on the source side there exists a shunted transmission line impedance, Z_{TL} [2, 4]. Accordingly, the input (Z_{IN}) impedance becomes:

$$Z_{IN} = R_{IN} + jX_{IN} = \frac{2Z_{TL}\left[(1+\alpha)^2 Z_{ANT}\right]}{2Z_{TL} + (1+\alpha)^2 Z_{ANT}} \qquad (0)$$

To achieve maximum power gain, Z_{IN} should be matched to the complex conjugate of the impedance of the RFID IC that is [5]:

$$Z_{IN} = Z_{IC}^{*} = R_{IC} - jX_{IC} \qquad (0)$$

B. Integrated T-match network

The antenna along with the integrated TMN is rendered into a microstrip planar design as shown in Fig. 2 below.

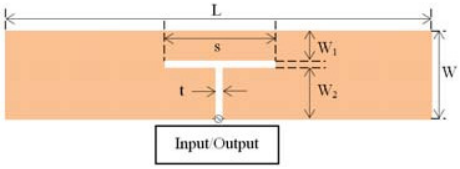

Fig. 2. A microstrip design of the antenna with the integrated TMN.

The integrated TMN design is advantageous because only four design parameters (*L, W, W_1*, and *s*) exist [1, 2]. It is a favorable matching technique as it provides a systematic means for synthesizing a matched antenna for RFID applications. This is in direct contrast to complex meandered RFID antenna designs which consist of a large amount of design parameters.

This work was supported by the National Science Foundation under grant ECCS 1711467.

C. *Determining the width (W) and length (L) through simulation*

An expression for the current division factor (α) as a function of Z_{ANT} can be derived by equating (2) and (3). Using ANSYS HFSS, a dipole is designed near the upper RFID band of 920 MHz with various widths, *W*. The length, *L*, is then swept within a defined range. The curves obtained are shown in Fig. 3 and they represent all possible solution combinations of the width, *W* and length, *L*, of the antenna with the integrated TMN.

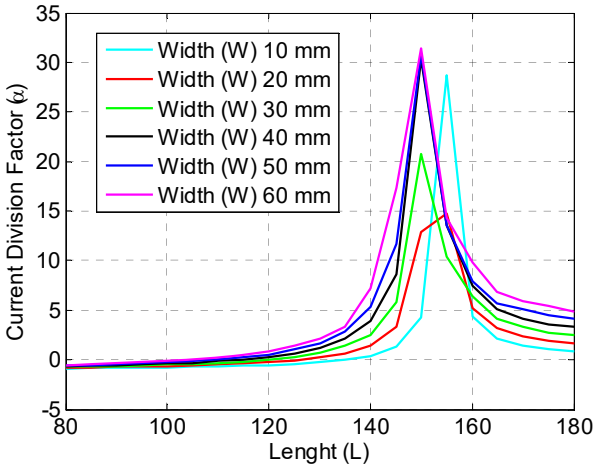

Fig. 3. Current division factor, *α*, vs. length, *L*, for various widths, *W*.

The judicious selection of the width (W) and length (L) will depend on the best match obtained at both the upper (920 MHz) and lower (904 MHz) operating frequencies of the RFID band. Furthermore, once the length (*L*) and width (*W*) are decided, the width (W_1) is obtained by (1).

III. Operating in the Freqeuncy Domain

The designed shift in frequency is achieved through lifting the antenna above a ground plane. This is done using a novel 3D printed 2 x 4 LCE array [3]. The array is placed under the antenna and above the ground plane. When heated, each flat element in the LCE array forms into a dome, refer to Fig. 4. As a result, the antenna is elevated from the ground plane, decreasing the parasitic capacitance, and increasing the resonant frequency [1]. The LCE array returns to the flat state upon removal of the heat stimulus.

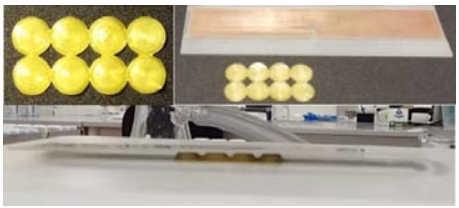

Fig. 4. (a) 3D printed 2 x 4 LCE array (upper left). (b) antenna with integrated TMN (upper right) (c) 3D LCE array actuating the antenna (bottom)

IV. Power Transmission Simulation

The length, *s*, refer to Fig. 2, is swept in ANSYS HFSS until the maximum power transfer (τ) is achieved when the antenna is elevated, at 920 MHz. The antenna is then lowered in reference to the ground plane to lower the resonant frequency of the antenna. The ideal length of *s* is 6 mm and provides a favorable match at both operating frequencies, refer to Fig. 5 below.

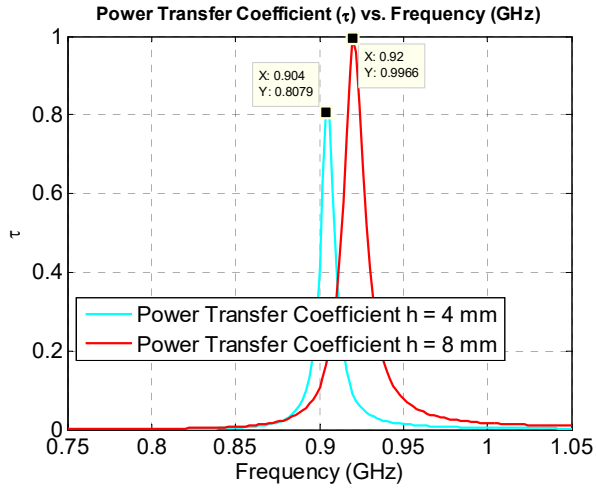

Fig. 5. RFID sensor's performance at operating frequencies 904 MHz (blue) and 920 MHz (red).

V. Conclusion

An innovative temperature sensor using RFID technology is proposed in this paper. The sensor consists of a dipole antenna with an integrated TMN above a ground plane. The sensor operates by shifting its operating frequency in the RFID band (from 904 MHz to 920 MHz) when the temperature is higher than a set value. This is achieved by using a novel 3D printed LCE array designed to actuate and increase the distance of the RFID antenna from the ground plane when the temperature is above a set value. This actuation is reversible, i.e., when the temperature decreases below this set value, the LCE array will return to original shape thereby bringing the antenna to its original position that is closer to the ground plane. The simulation shows that the sensor operates auspiciously at both 904 MHz and 920 MHz in the RFID band.

References

[1] R. Bhattacharyya, C. Floerkemeier, S. Sarma and D. Deavours, "RFID tag antenna based temperature sensing in the frequency domain," *2011 IEEE International Conference on RFID*, Orlando, FL, 2011, pp. 70-77.

[2] N. A. Mohammed, K. R. Demarest and D. D. Deavours, "Analysis and synthesis of UHF RFID antennas using the embedded T-match," *2010 IEEE International Conference on RFID (IEEE RFID 2010)*, Orlando, FL, 2010, pp. 230-236.

[3] C. P. Ambulo, J. J. Burroughs, J. M. Boothby, H. Kim, M. R. Shankar, and T. H. Ware. "Four-dimensional Printing of Liquid Crystal Elastomers." *ACS Applied Materials & Interfaces*, vol. 9, no. 42, pp. 37332–37339, Nov. 2017.

[4] C. Balanis, Antenna Theory - Analysis and Design, 3rd ed. Hoboken, NJ: John Wiley & Sons, pp. 531-532.

[5] D. Pozar, Microwave engineering, 4th ed. Hoboken, NJ: Wiley, 2012, pp. 77-78.